
Three-dimensional MHD Hybrid Nanofluid Flow Between Two Vertical Porous Plates Moving In Opposite Directions *

3.1 INTRODUCTION

The theoretical and experimental survey on nanofluids, the efficient energy transport fluids describes their enormous interpretations and implications including heat exchangers and electronic devices. The strengthening in thermophysical properties of nanofluids adjudged, hybrid nanofluid attained much attention. The synergic effects improve thermal qualities and potential utilities of nanofluid, beneficial in the industrial area such as nuclear system cooling, thermal energy generating system, hot rolling, solar energy systems, etc.

The present chapter aims to analytically explore the three-dimensional convective hydromagnetic hybrid nanofluid (with suspended Al_2O_3 and Fe_3O_4 nanoparticles) flow between two oppositely moving vertical porous plates. Governing equations are solved using the perturbation technique and the consequence of effectual

*Published in Heat Transfer (Wiley), 2021;50(7); 6548-6571

parameters on velocity and temperature profiles are analyzed with aid of graphs using MATLAB software. The rate of heat transfer is statistically scrutinized using response surface methodology and sensitivity analysis.

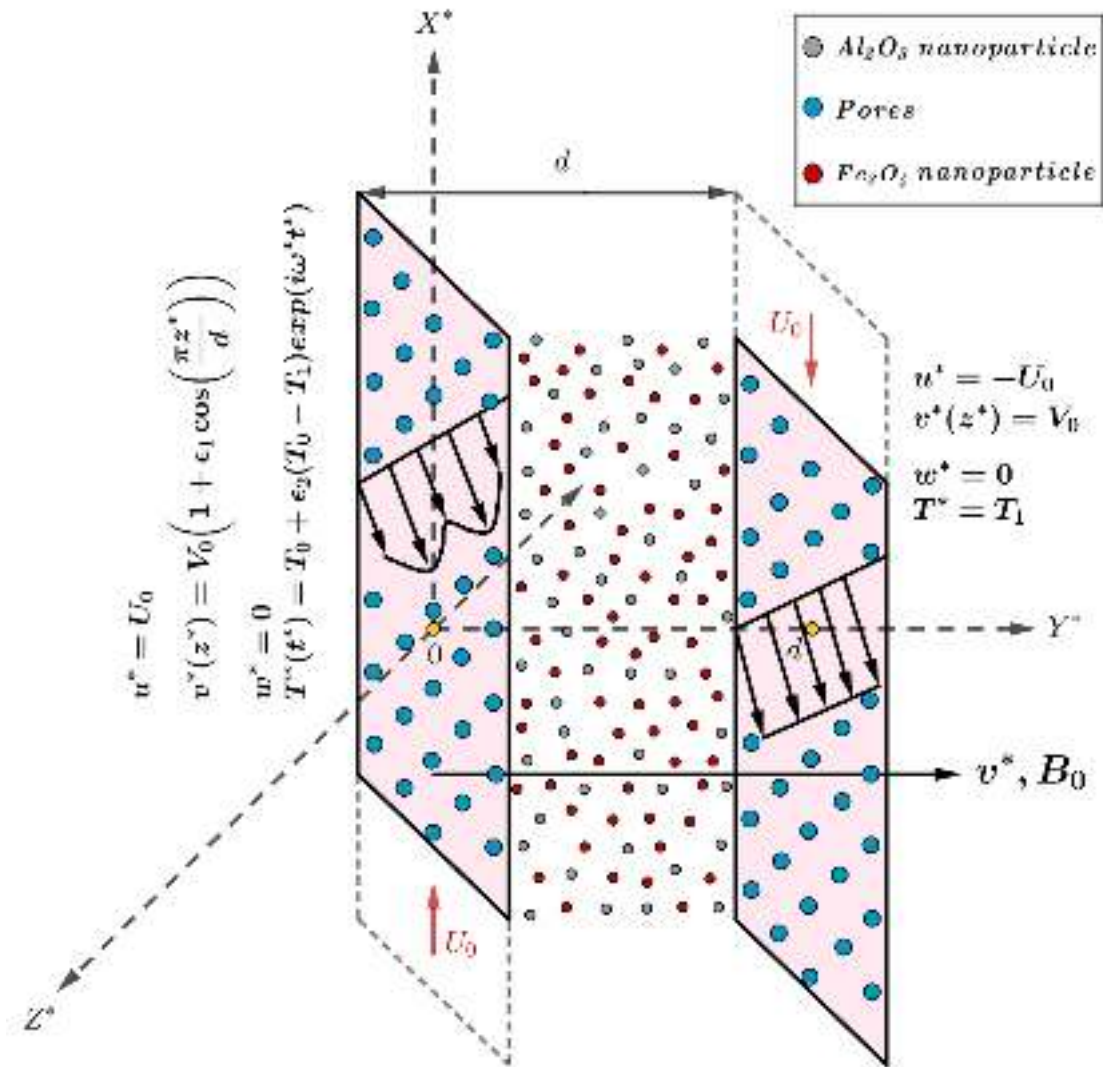


Figure 3.1: Physical configuration

3.2 MATHEMATICAL FORMULATION

An unsteady convective hybrid nanofluid flow between two vertical porous plates involving a magnetic field (of uniform strength, B_0 applied normally to the plane of the plate) is considered (see Figure 3.1). The problem is developed utilizing the following conditions:

1. Parallel plates are traveling in different directions with uniform velocities.

2. The upward and downward moving plates are subjected to transverse sinusoidal injection velocity and constant suction velocity, respectively.
3. Induced magnetic field has been neglected due to the assumption of a small magnetic Reynolds number.

4. The injection velocity distribution is of the form:

$$v^*(z^*) = V_0(1 + \varepsilon_1 \cos(\pi z^*/d))$$

5. Without loss of generality, the distance d between the plates is taken equal to the wavelength of the injection velocity.

6. The temperature of the downward moving plate is at constant temperature T_1 and that of the upward moving plate fluctuating with time is given as:

$$T^*(t^*) = T_0 + \varepsilon_2(T_0 - T_1)e^{i\omega^*t^*}$$

Utilizing Boussinesq's approximation and the above assumptions, governing equations (referred from (Singh & Mathew, 2009b)) are given by:

$$\frac{\partial v^*}{\partial y^*} + \frac{\partial w^*}{\partial z^*} = 0 \quad (3.2.1)$$

$$\begin{aligned} \frac{\partial u^*}{\partial t^*} + v^* \frac{\partial u^*}{\partial y^*} + w^* \frac{\partial u^*}{\partial z^*} = -\frac{1}{\rho_{hnf}} \left[\frac{\partial p^*}{\partial x^*} - \mu_{hnf} \left(\frac{\partial^2 u^*}{\partial y^{*2}} + \frac{\partial^2 u^*}{\partial z^{*2}} \right) + \sigma_{hnf} B_0^2 u^* \right] + \\ g\beta_{hnf}(T^* - T_1) \end{aligned} \quad (3.2.2)$$

$$\frac{\partial v^*}{\partial t^*} + v^* \frac{\partial v^*}{\partial y^*} + w^* \frac{\partial v^*}{\partial z^*} = -\frac{1}{\rho_{hnf}} \left[\frac{\partial p^*}{\partial y^*} - \mu_{hnf} \left(\frac{\partial^2 v^*}{\partial y^{*2}} + \frac{\partial^2 v^*}{\partial z^{*2}} \right) \right] \quad (3.2.3)$$

$$\frac{\partial w^*}{\partial t^*} + v^* \frac{\partial w^*}{\partial y^*} + w^* \frac{\partial w^*}{\partial z^*} = -\frac{1}{\rho_{hnf}} \left[\frac{\partial p^*}{\partial z^*} - \mu_{hnf} \left(\frac{\partial^2 w^*}{\partial y^{*2}} + \frac{\partial^2 w^*}{\partial z^{*2}} \right) + \sigma_{hnf} B_0^2 w^* \right] \quad (3.2.4)$$

$$\frac{\partial T^*}{\partial t^*} + v^* \frac{\partial T^*}{\partial y^*} + w^* \frac{\partial T^*}{\partial z^*} = \frac{K_{hnf}}{(\rho C_p)_{hnf}} \left[\frac{\partial^2 T^*}{\partial y^{*2}} + \frac{\partial^2 T^*}{\partial z^{*2}} \right] \quad (3.2.5)$$

subject to the boundary conditions:

$$\left. \begin{aligned} y^* = 0, u^* = U_0, v^*(z^*) = V_0(1 + \varepsilon_1 \cos \frac{\pi z^*}{d}), w^* = 0, \\ T^*(t^*) = T_0 + \varepsilon_2(T_0 - T_1)e^{i\omega^* t^*}, \\ y^* = d, u^* = -U_0, v^*(z^*) = V_0, w^* = 0, T^* = T_1 \end{aligned} \right\} \quad (3.2.6)$$

Hybrid nanofluid model used is

Effective Dynamic Viscosity:

$$C_1 = \frac{\mu_f}{\mu_{hnf}} = (1 - \phi_1)^{2.5}(1 - \phi_2)^{2.5}$$

Effective Density:

$$C_2 = \frac{\rho_{hnf}}{\rho_f} = (1 - \phi_2) \left[1 - \phi_1 + \phi_1 \left(\frac{\rho_{s1}}{\rho_f} \right) \right] + \phi_2 \left(\frac{\rho_{s2}}{\rho_f} \right)$$

Effective Electrical Conductivity:

$$C_3 = \frac{\sigma_{hnf}}{\sigma_f} = 1 + \frac{3 \left(\frac{\phi_1 \sigma_1 + \phi_2 \sigma_2}{\sigma_f} - (\phi_1 + \phi_2) \right)}{2 + \left(\frac{\phi_1 \sigma_1 + \phi_2 \sigma_2}{(\phi_1 + \phi_2) \sigma_f} \right) - \left(\frac{\phi_1 \sigma_1 + \phi_2 \sigma_2}{\sigma_f} - (\phi_1 + \phi_2) \right)}$$

Effective Coefficient Of Thermal Expansion:

$$C_4 = \frac{\beta_{hnf}}{\beta_f} = (1 - \phi_2) \left[1 - \phi_1 + \phi_1 \left(\frac{\beta_{s1}}{\beta_f} \right) \right] + \phi_2 \left(\frac{\beta_{s2}}{\beta_f} \right)$$

Effective Specific Heat:

$$C_5 = \frac{(\rho C_p)_{hnf}}{(\rho C_p)_f} = (1 - \phi_2) \left[1 - \phi_1 + \phi_1 \left(\frac{(\rho C_p)_{s1}}{(\rho C_p)_f} \right) \right] + \phi_2 \left(\frac{(\rho C_p)_{s2}}{(\rho C_p)_f} \right)$$

Effective Thermal Conductivity:

$$C_6 = \frac{K_{hnf}}{K_f}$$

where

$$\frac{K_{hnf}}{K_f} = \frac{K_{s2} + 2K_{nf} - 2\phi_2(K_{nf} - K_{s2})}{K_{s2} + 2K_{nf} + 2\phi_2(K_{nf} - K_{s2})}$$

and

$$\frac{K_{nf}}{K_f} = \frac{K_{s1} + 2K_f - 2\phi_1(K_f - K_{s1})}{K_{s1} + 2K_f + 2\phi_1(K_f - K_{s1})}$$

The following dimensionless quantities are introduced into equations (3.2.1) to (3.2.6) (except (3.2.2)),

$$y = \frac{y^*}{d}, z = \frac{z^*}{d}, t = t^*\omega^*, u = \frac{u^*}{U_0}, v = \frac{v^*}{V_0}, w = \frac{w^*}{V_0},$$

$$p = \frac{p^*}{\rho_{hnf}V_0^2}, \omega = \frac{\omega^*d^2}{\vartheta}, \theta = \frac{T^*-T_1}{T_0-T_1},$$

The reduced equations take the form:

$$\frac{\partial v}{\partial y} + \frac{\partial w}{\partial z} = 0 \quad (3.2.7)$$

$$\frac{\omega}{Re} \frac{\partial v}{\partial t} + v \frac{\partial v}{\partial y} + w \frac{\partial v}{\partial z} = -\frac{\partial p}{\partial y} + \frac{1}{C_1 C_2 Re} \left(\frac{\partial^2 v}{\partial y^2} + \frac{\partial^2 v}{\partial z^2} \right) \quad (3.2.8)$$

$$\frac{\omega}{Re} \frac{\partial w}{\partial t} + v \frac{\partial w}{\partial y} + w \frac{\partial w}{\partial z} = -\frac{\partial p}{\partial z} + \frac{1}{C_1 C_2 Re} \left(\frac{\partial^2 w}{\partial y^2} + \frac{\partial^2 w}{\partial z^2} \right) - \frac{C_3}{C_2 Re} H^2 w \quad (3.2.9)$$

$$\frac{\omega}{Re} \frac{\partial \theta}{\partial t} + v \frac{\partial \theta}{\partial y} + w \frac{\partial \theta}{\partial z} = \frac{C_6}{C_5 Pr Re} \left(\frac{\partial^2 \theta}{\partial y^2} + \frac{\partial^2 \theta}{\partial z^2} \right) \quad (3.2.10)$$

Equation (3.3.2) permutes to the following cases:

Case 1: Magnetic Field is applied on the upward moving plate (at $y=0$)

$$\frac{\omega}{Re} \frac{\partial u}{\partial t} + v \frac{\partial u}{\partial y} + w \frac{\partial u}{\partial z} = \frac{1}{C_1 C_2 Re} \left(\frac{\partial^2 u}{\partial y^2} + \frac{\partial^2 u}{\partial z^2} \right) - \frac{C_3}{C_2 Re} H^2 (u - 1) + C_4 Gr Re \theta \quad (3.2.11)$$

Case 2: Magnetic Field is applied on the downward moving plate (at $y=1$)

$$\frac{\omega}{Re} \frac{\partial u}{\partial t} + v \frac{\partial u}{\partial y} + w \frac{\partial u}{\partial z} = \frac{1}{C_1 C_2 Re} \left(\frac{\partial^2 u}{\partial y^2} + \frac{\partial^2 u}{\partial z^2} \right) - \frac{C_3}{C_2 Re} H^2 (u + 1) + C_4 Gr Re \theta \quad (3.2.12)$$

The reduced boundary conditions take the form:

$$\left. \begin{aligned} y = 0, u = 1, v(z) = 1 + \varepsilon_1 \cos \pi z, w = 0, \theta = 1 + \varepsilon_2 e^{it} \\ y = 1, u = -1, v = 1, w = 0, \theta = 0 \end{aligned} \right\} \quad (3.2.13)$$

3.3 METHOD OF SOLUTION

The reduced forms of the governing equations are resolved using the perturbation method. For this, let $\varepsilon = \min \{\varepsilon_1, \varepsilon_2\}$ be very small and suppose that solution is of the format

$$f(y, z, t) = f_0(y) + \varepsilon f_1(y, z, t) + O(\varepsilon^2) \quad (3.3.1)$$

3.3.1 Steady Flow Solution

Letting $\varepsilon = 0$, the current problem narrows to a steady two dimensional flow which is governed by the ensuing equations:

Case 1: Magnetic Field is applied on the upward moving plate (at $y=0$)

$$u_0'' - C_1 C_2 Re u_0' - C_1 C_3 H^2 (u_0 - 1) + C_1 C_2 C_4 Re^2 Gr \theta_0 = 0 \quad (3.3.2)$$

Case 2: Magnetic Field is applied on the downward moving plate (at $y=1$)

$$u_0'' - C_1 C_2 Re u_0' - C_1 C_3 H^2 (u_0 + 1) + C_1 C_2 C_4 Re^2 Gr \theta_0 = 0 \quad (3.3.3)$$

with $v_0 = 1, w_0 = 0, p_0 = \text{a constant}$ and

$$\theta_0'' - \frac{C_5 Pr Re}{C_6} \theta_0' = 0 \quad (3.3.4)$$

where prime notates the derivative with respect to y .

The analogous boundary conditions take the form:

$$\left. \begin{aligned} y = 0, u_0 = 1, \theta_0 = 1 \\ y = 1, u_0 = -1, \theta_0 = 0 \end{aligned} \right\} \quad (3.3.5)$$

Solving equations (3.3.2) to (3.3.4) with respect to (3.3.5) yields:

$$\theta_0 = \frac{1}{e^{a_1} - 1}(e^{a_1} - e^{a_1 y}) \quad (3.3.6)$$

Case 1: Magnetic Field is applied on the upward moving plate (at $y=0$)

$$u_0 = \frac{1}{e^{b_2} - e^{b_1}}[(\alpha_1 e^{b_2} - \beta_1)e^{b_1 y} + (\beta_1 - \alpha_1 e^{b_1})e^{b_2 y}] + A_1 e^{a_1 y} + A_2 + 1 \quad (3.3.7)$$

Case 2: Magnetic Field is applied on the downward moving plate (at $y=1$)

$$u_0 = \frac{1}{e^{b_2} - e^{b_1}}[((\alpha_1 + 2)e^{b_2} - (\beta_1 + 2))e^{b_1 y} + ((\beta_1 + 2) - (\alpha_1 + 2)e^{b_1})e^{b_2 y}] + A_1 e^{a_1 y} + A_2 - 1 \quad (3.3.8)$$

3.3.2 Cross Flow Solution

Letting $\varepsilon \neq 0$ applying equation (3.3.1) into equations (3.2.7) - (3.2.9) and equating like powers of ε and ignoring the higher powers of ε^2 , the following equations are derived:

$$\frac{\partial v_1}{\partial y} + \frac{\partial w_1}{\partial z} = 0 \quad (3.3.9)$$

$$\frac{\omega}{Re} \frac{\partial v_1}{\partial t} + \frac{\partial v_1}{\partial y} = -\frac{\partial p_1}{\partial y} + \frac{1}{C_1 C_2 Re} \left[\frac{\partial^2 v_1}{\partial y^2} + \frac{\partial^2 v_1}{\partial z^2} \right] \quad (3.3.10)$$

$$\frac{\omega}{Re} \frac{\partial w_1}{\partial t} + \frac{\partial w_1}{\partial y} = -\frac{\partial p_1}{\partial z} + \frac{1}{C_1 C_2 Re} \left[\frac{\partial^2 w_1}{\partial y^2} + \frac{\partial^2 w_1}{\partial z^2} \right] - \frac{C_3}{C_2 Re} H^2 w_1 \quad (3.3.11)$$

Corresponding boundary conditions are

$$\left. \begin{aligned} y = 0, v_1 = \cos \pi z, w_1 = 0 \\ y = 1, v_1 = 0, w_1 = 0 \end{aligned} \right\} \quad (3.3.12)$$

These are the linear partial differential equations reporting the three-dimensional cross flow which are independent of the temperature field and the main flow com-

ponent. The solutions for v_1, w_1, p_1 are assumed to be of the form:

$$v_1(y, z, t) = v_{11}(y)e^{it} + v_{12}(y) \cos \pi z \quad (3.3.13)$$

$$w_1(y, z, t) = -(zv_{11}'(y)e^{it} + \frac{1}{\pi}v_{12}'(y) \sin \pi z) \quad (3.3.14)$$

$$p_1(y, z, t) = p_{11}(y)e^{it} + p_{12}(y) \cos \pi z \quad (3.3.15)$$

where prime notates the derivative with respect to y . Expressions (3.3.13) and (3.3.14) have been chosen so that the equation of continuity (3.3.9) is trivially satisfied. Applying these into equations (3.3.10) and (3.3.11) and employing the boundary condition (3.3.12), the solutions for v_1, w_1, p_1 are obtained as:

$$v_1 = \frac{1}{D} \sum_{i=1}^4 D_i e^{r_i y} \cos \pi z \quad (3.3.16)$$

$$w_1 = -\frac{1}{\pi D} \sum_{i=1}^4 r_i D_i e^{r_i y} \sin \pi z \quad (3.3.17)$$

$$p_1 = -\frac{1}{C_1 C_2 Re \pi^2 D} \sum_{i=1}^4 D_i (r_i^3 - C_1 C_2 Re r_i^2 - (C_1 C_3 H^2 + \pi^2) r_i) e^{r_i y} \cos \pi z \quad (3.3.18)$$

3.3.3 Temperature Field

Comparably letting $\varepsilon \neq 0$, applying equation (3.3.1) to equation (3.2.10) and comparing like powers of ε , the equation for temperature field is given by:

$$\frac{\omega}{Re} \frac{\partial \theta_1}{\partial t} + \frac{\partial \theta_1}{\partial y} = \frac{C_6}{C_5 Pr Re} \left(\frac{\partial^2 \theta_1}{\partial y^2} + \frac{\partial^2 \theta_1}{\partial z^2} \right) \quad (3.3.19)$$

with

$$\left. \begin{array}{l} y = 0, \theta_1 = e^{it} \\ y = 1, \theta_1 = 0, \end{array} \right\} \quad (3.3.20)$$

Equation (3.3.19) along with equation (3.3.20) is solved with a supposition that the solution is of the format:

$$\theta_1(y, z, t) = \theta_{11}e^{it} + \theta_{12} \cos \pi z \quad (3.3.21)$$

Substituting equation (3.3.21) into (3.3.19), one can obtain

$$\theta_{11}'' - \frac{C_5 Pr Re}{C_6} \theta_{11}' - \frac{C_5 Pr \omega i}{C_6} \theta_{11} = 0 \quad (3.3.22)$$

$$\theta_{12}'' - \frac{C_5 Pr Re}{C_6} \theta_{12}' - \pi^2 \theta_{12} = 0 \quad (3.3.23)$$

with

$$\left. \begin{aligned} y = 0, \theta_{11} = 1, \theta_{12} = 0 \\ y = 1, \theta_{11} = 0, \theta_{12} = 0 \end{aligned} \right\} \quad (3.3.24)$$

Resolving equations (3.3.22) and (3.3.23) utilizing equation (3.3.24), the solution is given by:

$$\theta_1(y, z, t) = \frac{1}{e^{a_3} - e^{a_2}} (e^{a_3} e^{a_2 y} - e^{a_2} e^{a_3 y}) e^{it} \quad (3.3.25)$$

3.3.4 Main Flow Solution

Letting $\varepsilon \neq 0$, the first order equation for the main flow deduced with the help of equation (3.3.1) and equating like powers of ε is given by:

$$\frac{\omega}{Re} \frac{\partial u_1}{\partial t} + \frac{\partial u_1}{\partial y} + v_1 u_0' = \frac{1}{C_1 C_2 Re} \left(\frac{\partial^2 u_1}{\partial y^2} + \frac{\partial^2 u_1}{\partial z^2} \right) - \frac{C_3}{C_2 Re} H^2 u_1 + C_4 Gr Re \theta_1 \quad (3.3.26)$$

with

$$\left. \begin{aligned} y = 0, \quad u_1 = 0 \\ y = 1, \quad u_1 = 0 \end{aligned} \right\} \quad (3.3.27)$$

Suppose the solution is of the format:

$$u_1(y, z, t) = u_{11}e^{it} + u_{12} \cos \pi z \quad (3.3.28)$$

Applying equation (3.3.28) in equation (3.3.26) and comparing like powers of ε :

$$u_{11}'' - C_1 C_2 Re u_{11}' - (C_1 C_2 \omega i + C_1 C_3 H^2) u_{11} = -C_1 C_2 C_4 Re^2 Gr \theta_{11} \quad (3.3.29)$$

$$u_{12}'' - C_1 C_2 Re u_{12}' - (\pi^2 + C_1 C_3 H^2) u_{12} = C_1 C_2 Re v_{12} u_0' \quad (3.3.30)$$

with

$$\left. \begin{aligned} y = 0, \quad u_{11} = 0, \quad u_{12} = 0 \\ y = 1, \quad u_{11} = 0, \quad u_{12} = 0 \end{aligned} \right\} \quad (3.3.31)$$

Resolving equations (3.3.29) and (3.3.30) utilizing equation (3.3.31), the solution is derived as:

Case 1: Magnetic Field is applied on the upward moving plate (at $y=0$)

$$u_1(y, z, t) = \left\{ \begin{aligned} & \frac{1}{e^{b_4} - e^{b_3}} [(\alpha_2 e^{b_4} - \beta_2) e^{b_3 y} + (\beta_2 - \alpha_2 e^{b_3}) e^{b_4 y}] + \\ & A_3 e^{a_2 y} + A_4 e^{a_3 y} \end{aligned} \right\} e^{it} + \left\{ \begin{aligned} & \frac{1}{e^{b_6} - e^{b_5}} [(\alpha_3 e^{b_6} - \beta_3) e^{b_5 y} + (\beta_3 - \alpha_3 e^{b_5}) e^{b_6 y}] + \\ & \sum_{i=1}^4 A_{i1} e^{(r_i + b_1) y} + A_{i2} e^{(r_i + b_2) y} + A_{i3} e^{(r_i + a_1) y} \end{aligned} \right\} \cos \pi z \quad (3.3.32)$$

Case 2: Magnetic Field is applied on the downward moving plate (at $y=1$)

$$u_1(y, z, t) = \left\{ \begin{aligned} & \frac{1}{e^{b_4} - e^{b_3}} [(\alpha_2 e^{b_4} - \beta_2) e^{b_3 y} + (\beta_2 - \alpha_2 e^{b_3}) e^{b_4 y}] + \\ & A_3 e^{a_2 y} + A_4 e^{a_3 y} \end{aligned} \right\} e^{it} + \left\{ \begin{aligned} & \frac{1}{e^{b_6} - e^{b_5}} [(\alpha_4 e^{b_6} - \beta_4) e^{b_5 y} + (\beta_4 - \alpha_4 e^{b_5}) e^{b_6 y}] + \\ & \sum_{i=1}^4 B_{i1} e^{(r_i + b_1) y} + B_{i2} e^{(r_i + b_2) y} + B_{i3} e^{(r_i + a_1) y} \end{aligned} \right\} \cos \pi z \quad (3.3.33)$$

3.4 PHYSICAL QUANTITIES

Physical quantities like drag coefficient (Cf) and Nusselt number (Nu) measuring surface drag and rate of heat transfer, respectively are given by:

Case 1: Magnetic Field is applied on the upward moving plate (at $y=0$)

$$Cf = \frac{d}{\mu_f U_0} \left| \mu_{hmf} \left(\frac{du^*}{dy^*} \right)_{y^*=d} \right| = \frac{1}{C_1} \left| \left(\frac{du_0}{dy} \right)_{y=1} + \varepsilon \left(\frac{du_1}{dy} \right)_{y=1} \right| \quad (3.4.1)$$

Case 2: Magnetic Field is applied on the downward moving plate (at $y=1$)

$$Cf = \frac{d}{\mu_f U_0} \left| \mu_{hmf} \left(\frac{du^*}{dy^*} \right)_{y^*=d} \right| = \frac{1}{C_1} \left| \left(\frac{du_0}{dy} \right)_{y=1} + \varepsilon \left(\frac{du_1}{dy} \right)_{y=1} \right| \quad (3.4.2)$$

$$Nu = \frac{d}{K_f(T_0 - T_1)} \left| K_{hnf} \left(\frac{dT^*}{dy^*} \right)_{y^*=d} \right| = C_6 \left| \left(\frac{d\theta_0}{dy} \right)_{y=0} + \varepsilon \left(\frac{d\theta_1}{dy} \right)_{y=0} \right| \quad (3.4.3)$$

3.5 RESULTS AND DISCUSSION

The significance of effectual parameters on velocity (u), surface drag (Cf) and temperature (θ) profiles are depicted through Figures 3.2 - 3.13. The physical properties of nanoparticles (Al_2O_3 and Fe_3O_4) and the conventional fluid (water) are identified in Table 3.1. $\phi_1 = 0.1, \phi_2 = 0.1, \omega = 10, Re = 1, H = 2, Pr = 7, Gr = 7$ and $t = \pi/2$ are the base values of parameters employed (unless specified) throughout the analysis. Further, the validation of the obtained results is achieved through a comparative study with the previous work (Neethu, Areekara, & Mathew, 2021) (see Table 3.2) and a good agreement is noted.

Figure 3.2 explains the positive effect of Grashof number (Gr) on u meaning that an augmentation in Gr will increase the velocity. Physically, on magnifying Gr the buoyancy forces becomes prominent which results in ascending the velocity profile. Figure 3.3 manifests the consequence of Hartmann number (H) on u . The introduction of a magnetic field produces a drag force (Lorentz force) which sets up an opposite reaction on upward and downward moving plates. On varying H , it is noted that u ascends on upward moving plate whereas u descends on the downward-moving plate. The negative influence of the volume fraction of nanoparticles (ϕ_1 and ϕ_2) on u is elucidated in Figures 3.4 and 3.5, respectively. This decrease in velocity can be physically attributed to the fact that increasing the volume fraction of nanoparticles swells the viscosity of hybrid nanoliquid which causes a drop in velocity. The influence of injection/suction parameter (Re) on u is depicted in Figure 3.6. Velocity profile experiences an exponential augmentation when Re values are improved.

Figure 3.7 and 3.8 reveals that intensification in the volume fraction of nanoparticles brings about a reduction in θ . The impact of Re on θ is displayed using Figure 3.9 and it is noted that Re causes an improvement in θ . Physically, this increase in temperature can be associated with the fact that with increasing Re values the heated nanoparticles enter the opposite moving plates and the cold nanoparticles exit the opposite moving plates.

The parallel effect of effectual parameters on drag coefficient (Cf) on the up-

ward and downward-moving plates is illustrated in Figures 3.10 - 3.13 with the aid of three-dimensional surface plots. It is seen that surface drag ascends with ϕ_1, Re, H and Gr on the upward moving plate. Further, surface drag ascends with ϕ_1, Re , and Gr and descends with H on the downward moving plate.

3.6 STATISTICAL ANALYSIS

3.6.1 Response Surface Methodology (RSM)

RSM is a statistical approach employed in analyzing the conjoint impact of effectual parameters (independent variables) on the physical quantity of interest (response or dependent variable). In this problem, Nu is chosen as the response variable and nanoparticle volume fraction of Al_2O_3 ($0.02 \leq \phi_1 \leq 0.08$), nanoparticle volume fraction of Fe_3O_4 ($0.02 \leq \phi_2 \leq 0.08$) and injection/suction parameter ($1 \leq Re \leq 2$) are chosen as the influential parameters. Table 3.3 bespeaks the effective parameters and their levels. The general model (adopting central composite design) for response variables involving linear, interactive and quadratic terms is expressed by:

$$\text{Response} = \lambda_0 + \lambda_1 A + \lambda_2 B + \lambda_3 C + \lambda_4 AB + \lambda_5 BC + \lambda_6 AC + \lambda_7 A^2 + \lambda_8 B^2 + \lambda_9 C^2 \quad (3.6.1)$$

where $\lambda_i (i = 0, 1, \dots, 9)$ represents the regression coefficients. The experimental design and the response for the 20 runs (according to CCD) are given in Table 3.4.

The analysis of variable (ANOVA) table (Table 3.5) illustrates the efficiency of the estimated model. A parameter is claimed as significant if the corresponding p-value is less than 0.05. It is observed that the quadratic terms in ϕ_1 and ϕ_2 are not significant. Hence, they removed these terms from the model. The coefficient of determination (R^2) for the model is found to be 100% which boosts the model's accuracy.

The fitted quadratic model for Nu is given by:

$$Nu = 10.2645 - 0.07064\phi_1 - 0.0394\phi_2 + 3.403Re + 0.01807Re^2 + 0.0053\phi_1\phi_2 - 0.03258\phi_1Re - 0.0209\phi_2Re \quad (3.6.2)$$

The reliability of the estimated model for Nu is further clarified using residual plots (see Figure 3.14). All points in the normal probability plot are situated

beside a straight line with an insignificant deflection and the residual histogram is approximately bell-shaped confirming the normal nature of residuals. Furthermore, a maximum error of 0.005 can be observed from the fitted versus residual plot which also contributes to the accuracy of the model.

From equation (3.6.2), it can be inferred that ϕ_1 and ϕ_2 have a negative impact on Nu and Re has a positive effect on Nu . The parallel interaction of two parameters on Nu is graphed using surface and contour plots (see Figure 3.15) by fixing the third parameter at the medium level. From Figures 3.15 (a) - (c), it is perceived that Nu is highest for smaller values of ϕ_1 and ϕ_2 and larger values of Re .

3.6.2 Sensitivity Analysis

Sensitivity analysis is a statistical technique that measures the extent and nature of dependency exhibited by the effectual parameters on the physical quantity of interest. In other words, sensitivity analysis accounts for the variation induced by the augmenting parameter on the remaining effectual parameter. The sign of sensitivity (positive or negative) signifies the nature of the correlation between Nu and the influential parameters. Further, the magnitude of sensitivity indicates the intensity of the effect on Nu .

The quadratic model (in coded form) after neglecting the insignificant terms is given by:

$$Nu = 10.2645 - 0.07064 A - 0.0394 B + 3.403 C + 0.01807 C^2 + 0.0053 AB - 0.03258 AC - 0.0209 BC \quad (3.6.3)$$

Then the sensitivity functions are:

$$\frac{\partial Nu}{\partial A} = -0.07064 + 0.0053 B - 0.03258 C \quad (3.6.4)$$

$$\frac{\partial Nu}{\partial B} = -0.0394 + 0.0053 A - 0.0209 C \quad (3.6.5)$$

$$\frac{\partial Nu}{\partial C} = 3.403 + 0.03614 C - 0.03258 A - 0.0209 B \quad (3.6.6)$$

The sensitivity for Nu is tabulated in Table 3.6 keeping ϕ_1 in the medium level. It is noted that ϕ_1 and ϕ_2 exhibit negative sensitivity and Re exhibits a positive

sensitivity towards Nu . The sensitivity of Nu is also visualized using bar charts (Figure 3.16). It is seen that the results of sensitivity analysis are in perfect harmony with the results inferred using RSM. It is also noticed that Nu is most sensitive with Re .

3.7 CONCLUSION

The key observations are:

- Grashof number has a constructive effect on main flow velocity.
- Hartman number positively contributes towards the velocity profile on the upward moving plate and negatively contributes towards the velocity profile on the downward moving plate.
- Main flow velocity profile is higher when the magnetic field is applied on the upward-moving plate.
- Drag coefficient is directly proportional to the volume fraction of nanoparticles.
- Rate of heat transfer is the most sensitive parameter with injection/suction parameter.
- Augmentation of volume fraction of Al_2O_3 nanoparticles has more influence on the flow profiles.
- Surface drag coefficient ascends with augmenting Hartmann number on the upward moving plate and descends on the downward moving plate.
- Volume fraction of nanoparticles exhibits a destructive effect on heat transfer rate.

TABLES AND GRAPHS
Table 3.1: *Physical properties of nanoparticles and base fluid*

Physical Properties	H_2O	Al_2O_3	Fe_3O_4
ρ	997.1	3970	5180
C_p	4179	765	670
β	$21 * 10^{-5}$	$0.85 * 10^{-5}$	$1.3 * 10^{-5}$
σ	$5 * 10^{-2}$	$35 * 10^6$	25000
k	0.613	40	9.7

Table 3.2: *Comparison of Nu with augmenting Re values when $\phi_1 = 0, \phi_2 = 0, \Omega = 10, t = \pi/2, Pr = 7, Gr = 5$ and $H = 2$*

Re	Nu	
	(Neethu et al., 2021)	Present study
0.5	3.60681	3.60681
1	6.9976	6.9976
1.5	10.4771	10.4771
2	13.9665	13.9665
2.5	17.4835	17.4835

Table 3.3: *Effective parameter levels*

Parameter	Symbol	Levels		
		-1(low)	0(medium)	1(high)
ϕ_1	A	0.02	0.05	0.08
ϕ_2	B	0.02	0.05	0.08
Re	C	1	1.5	2

Table 3.4: *Experimental design with response*

Run	Coded values			Actual values			Response
	A	B	C	ϕ_1	ϕ_2	Re	Nu
1	-1	-1	-1	0.02	0.02	1	6.9437
2	1	-1	-1	0.08	0.02	1	6.8562
3	-1	1	-1	0.02	0.08	1	6.895
4	1	1	-1	0.08	0.08	1	6.8352
5	-1	-1	1	0.02	0.02	2	13.8524
6	1	-1	1	0.08	0.02	2	13.6411
7	-1	1	1	0.02	0.08	2	13.7266
8	1	1	1	0.08	0.08	2	13.53
9	-1	0	0	0.02	0.05	1.5	10.3412
10	1	0	0	0.08	0.05	1.5	10.19
11	0	-1	0	0.05	0.02	1.5	10.309
12	0	1	0	0.05	0.08	1.5	10.2216
13	0	0	-1	0.05	0.05	1	6.8773
14	0	0	1	0.05	0.05	2	13.6873
15	0	0	0	0.05	0.05	1.5	10.2646
16	0	0	0	0.05	0.05	1.5	10.2646
17	0	0	0	0.05	0.05	1.5	10.2646
18	0	0	0	0.05	0.05	1.5	10.2646
19	0	0	0	0.05	0.05	1.5	10.2646
20	0	0	0	0.05	0.05	1.5	10.2646

Table 3.5: ANOVA table

	Deg. Of freedom	Adj. sum of squares	Adj. mean squares	Regression Coeffi- cient	F-Value	p-Value
Model	9	115.884	12.876		924250	0
<i>Linear</i>	3	115.87	38.623		2772413	0
ϕ_1	1	0.05	0.05	-0.0706	3581.88	0
ϕ_2	1	0.016	0.016	-0.0394	1114.3	0
<i>Re</i>	1	115.804	115.804	3.403	8312544	0
<i>Square</i>	3	0.002	0.001		46	0
$\phi_1 * \phi_1$	1	0	0	0.00137	0.37	0.556
$\phi_2 * \phi_2$	1	0	0	0.00107	0.23	0.644
<i>Re * Re</i>	1	0.001	0.001	0.01807	64.47	0
<i>2-Way Interac- tion</i>	3	0.012	0.004		292.11	0
$\phi_1 * \phi_2$	1	0	0	0.0053	16.13	0.002
$\phi_1 * Re$	1	0.008	0.008	-0.0326	609.35	0
$\phi_2 * Re$	1	0.003	0.003	-0.0209	250.84	0
<i>Constant</i>				10.2645		
<i>Error</i>	10	0	0			
<i>Lack-of- Fit</i>	5	0	0		*	*
<i>Pure Er- ror</i>	5	0	0			
<i>Total</i>	19	115.884				
$R^2 = 100\%$			Adjusted $R^2 = 100\%$			

Table 3.6: *Sensitivity of response Nu when $A = 0$*

B	C	Sensitivity		
		$\frac{\partial Nu}{\partial A}$	$\frac{\partial Nu}{\partial B}$	$\frac{\partial Nu}{\partial C}$
	-1	-0.0434	-0.0185	3.3878
-1	0	-0.0759	-0.0394	3.4239
	1	-0.1085	-0.0603	3.46
	-1	-0.0381	-0.0185	3.3669
0	0	-0.0706	-0.0394	3.403
	1	-0.1032	-0.0603	3.4391
	-1	-0.0328	-0.0185	3.346
1	0	-0.0653	-0.0394	3.3821
	1	-0.0979	-0.0603	3.4182

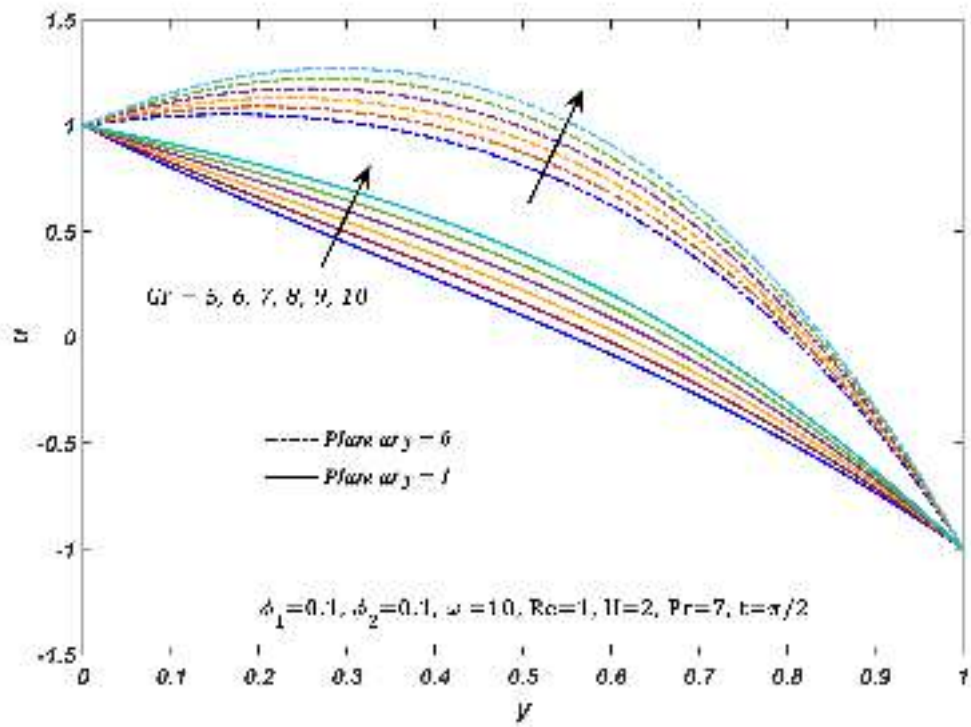


Figure 3.2: Variation in u with Gr

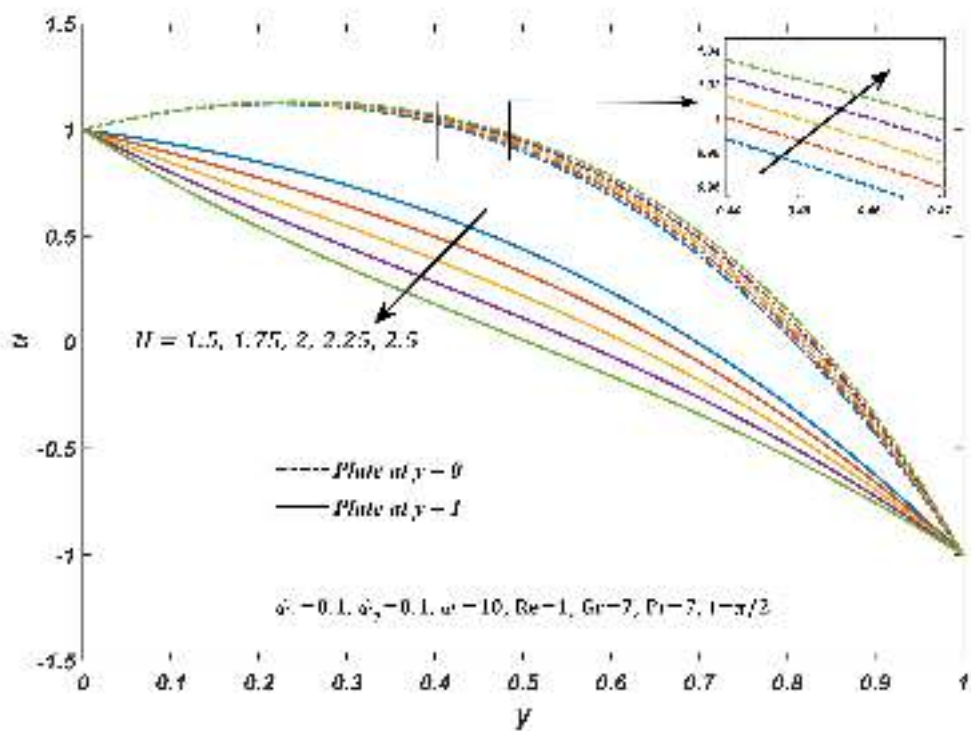


Figure 3.3: Variation in u with H

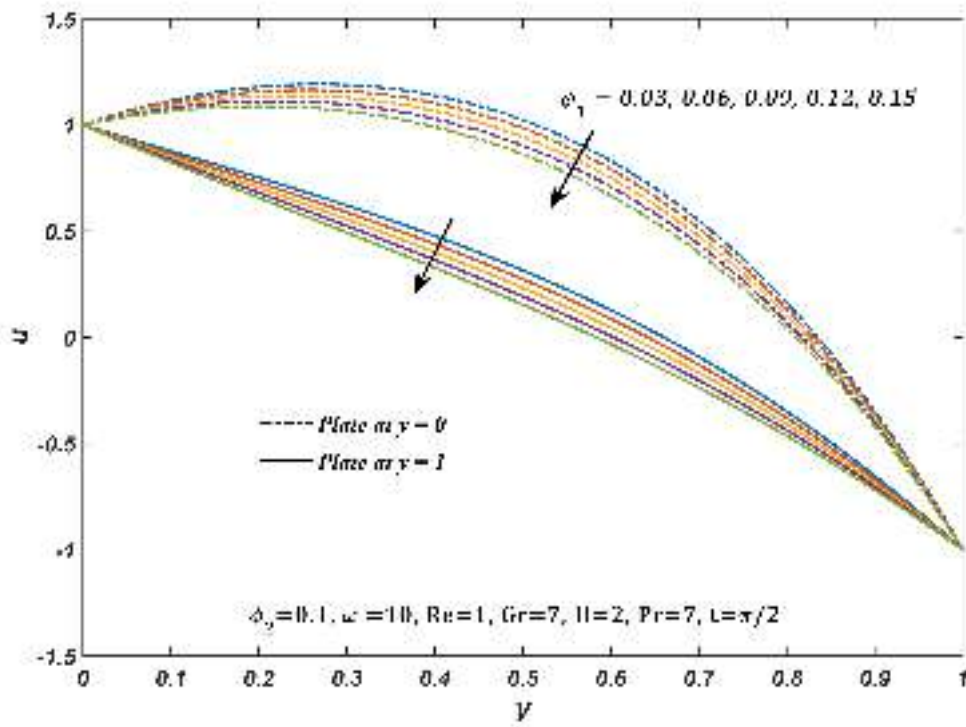


Figure 3.4: Variation in u with ϕ_1

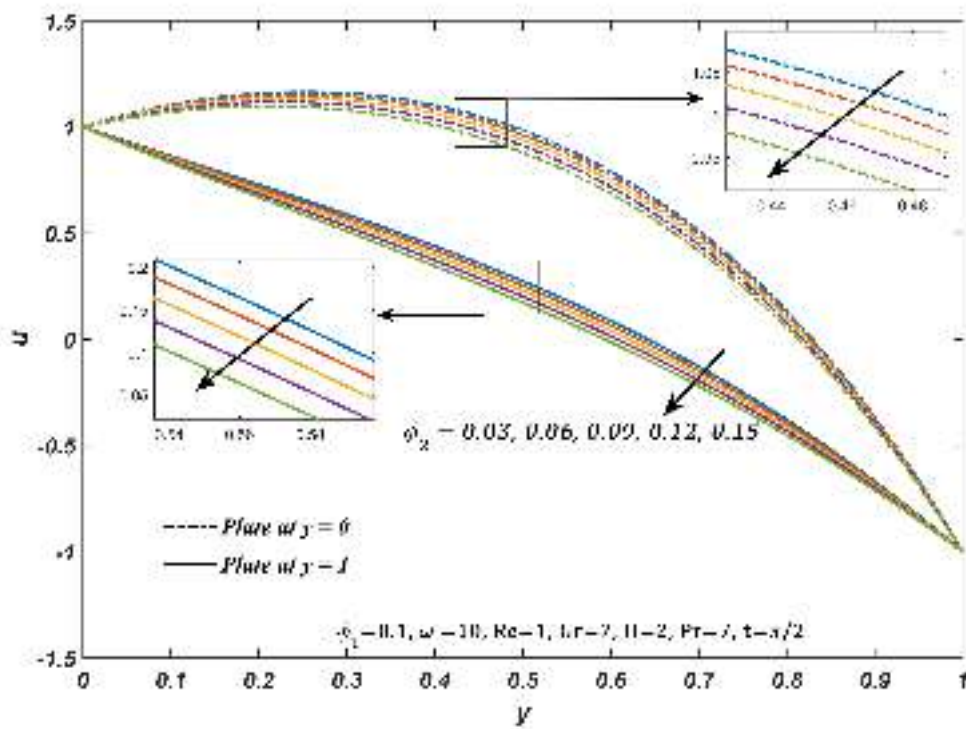


Figure 3.5: Variation in u with ϕ_2

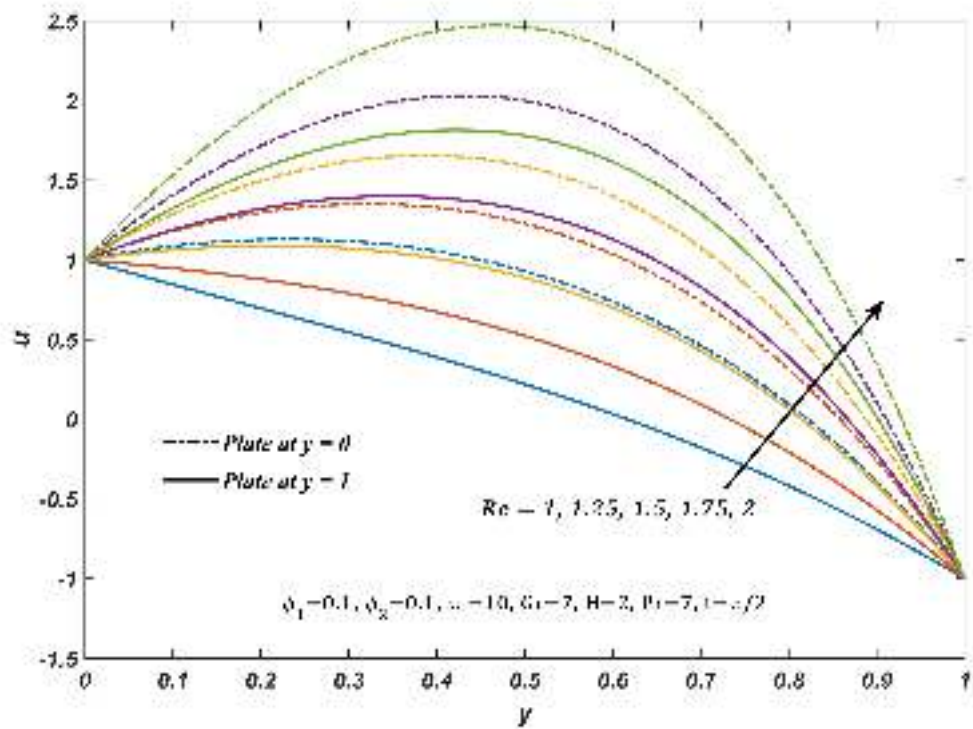


Figure 3.6: Variation in u with Re

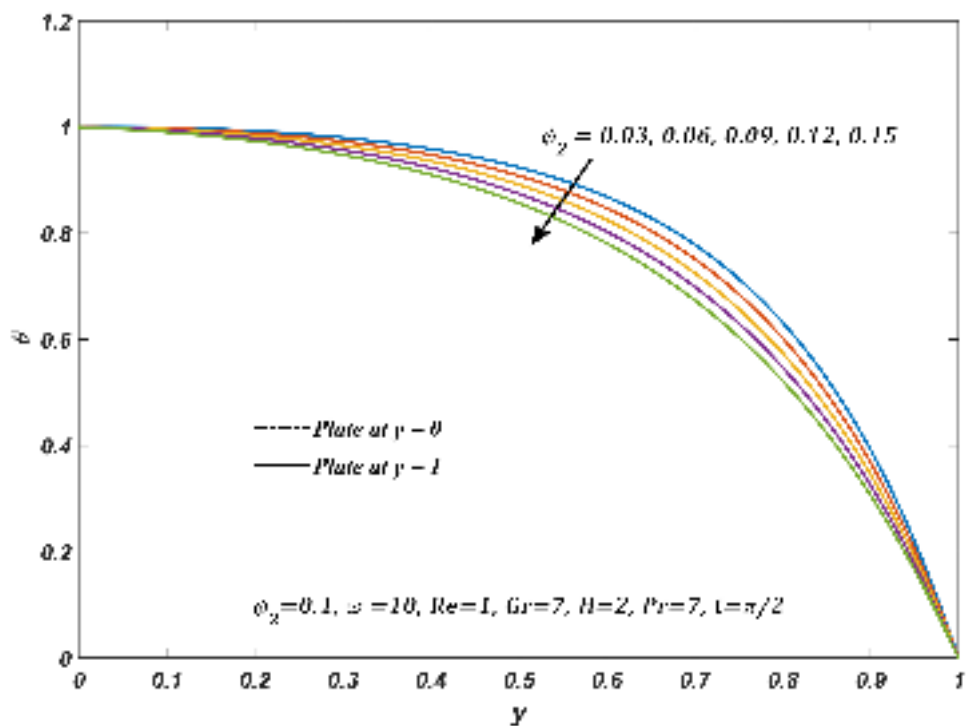


Figure 3.7: Variation in θ with ϕ_1

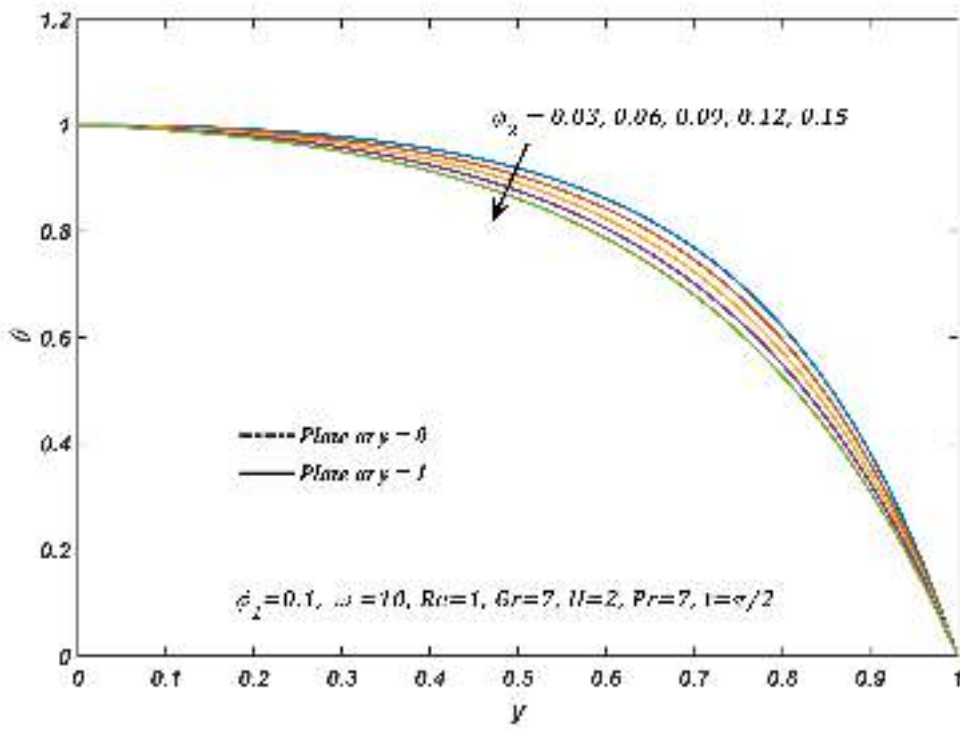


Figure 3.8: Variation in θ with ϕ_2

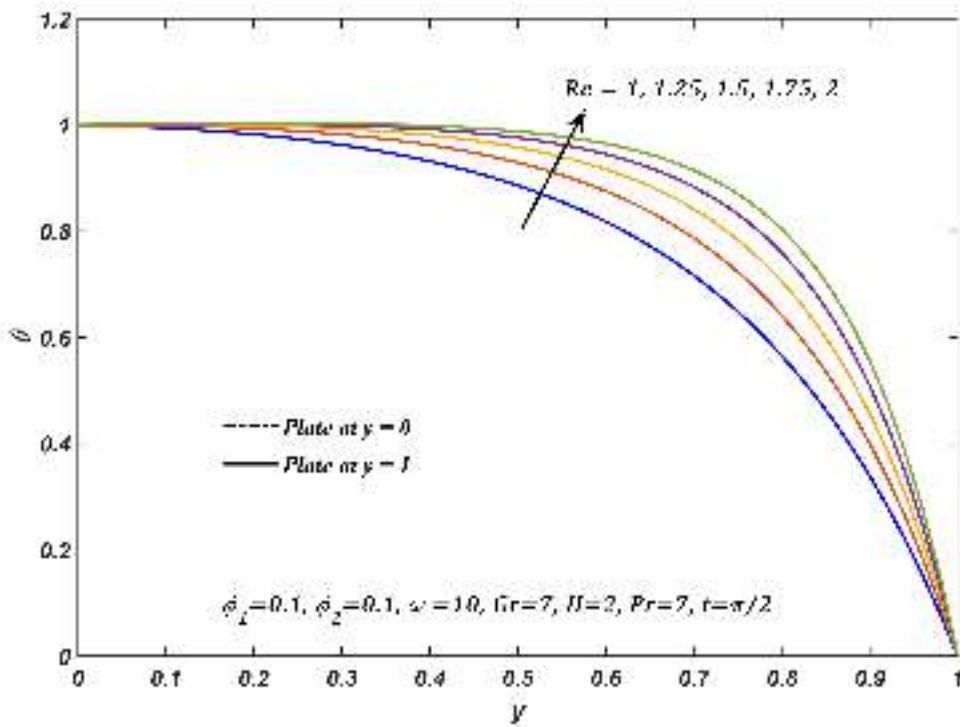


Figure 3.9: Variation in θ with Re

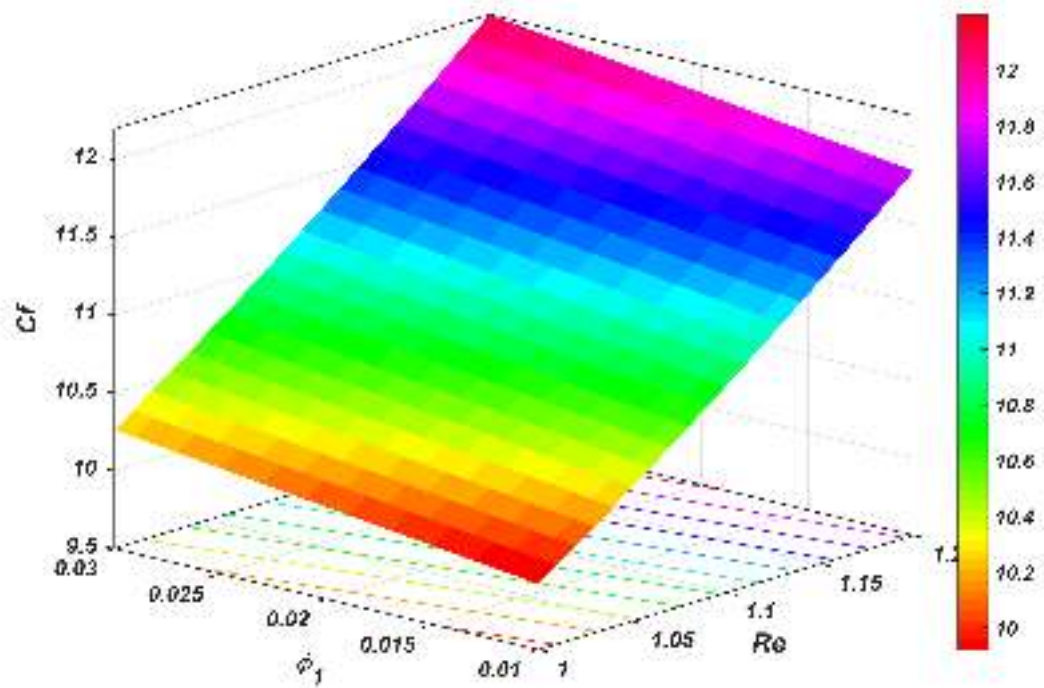


Figure 3.10: Variation in C_f with ϕ_1 and Re at $y = 0$

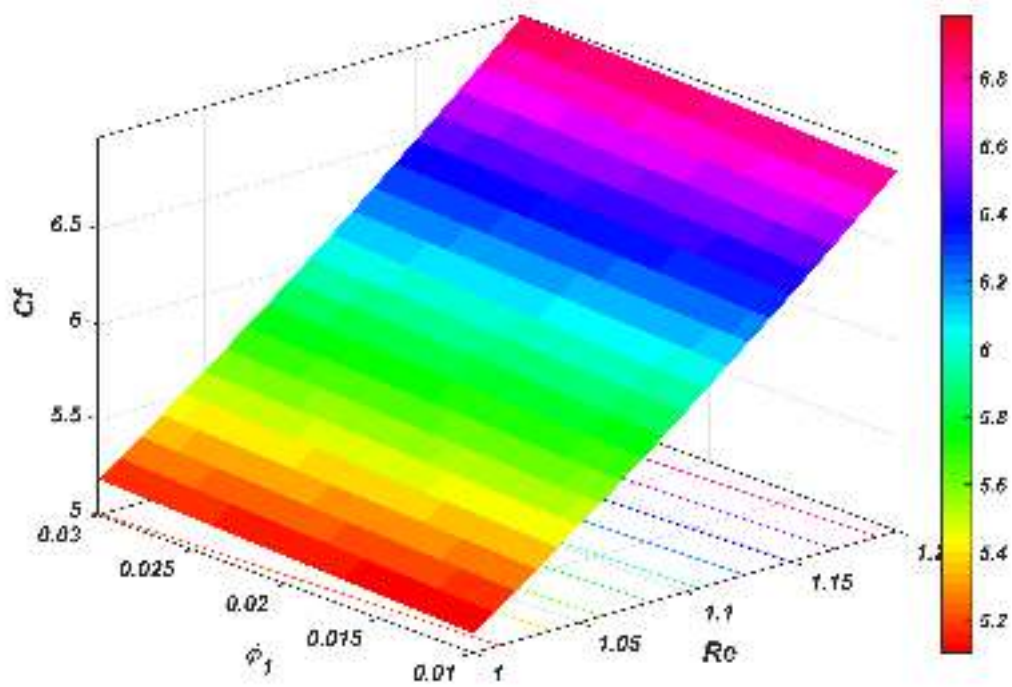


Figure 3.11: Variation in C_f with ϕ_1 and Re at $y = 1$

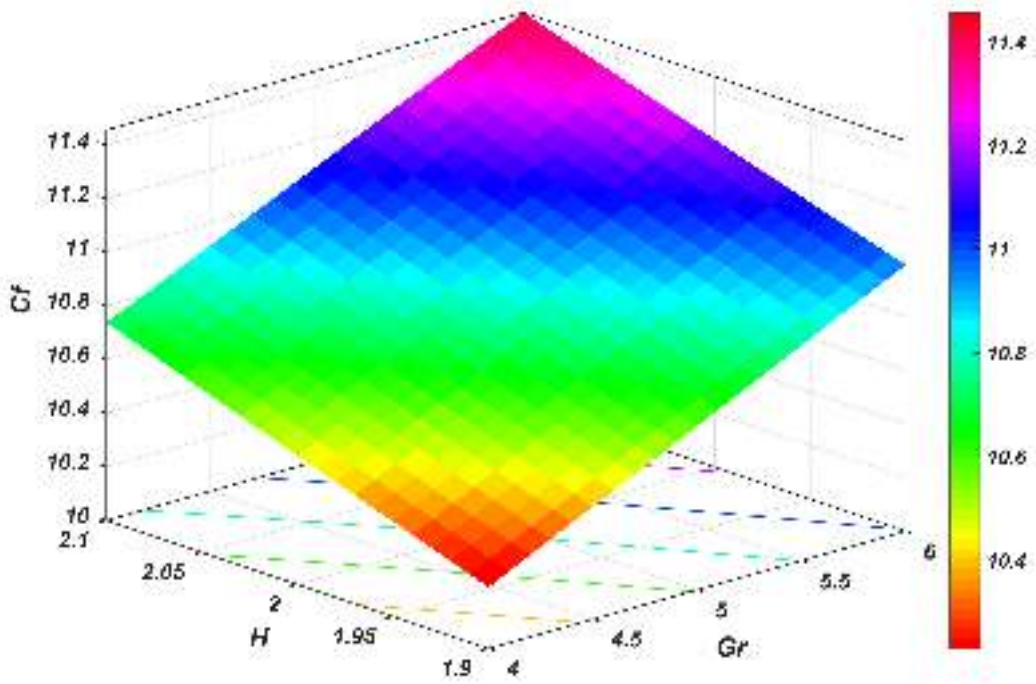


Figure 3.12: Variation in C_f with Gr and H at $y = 0$

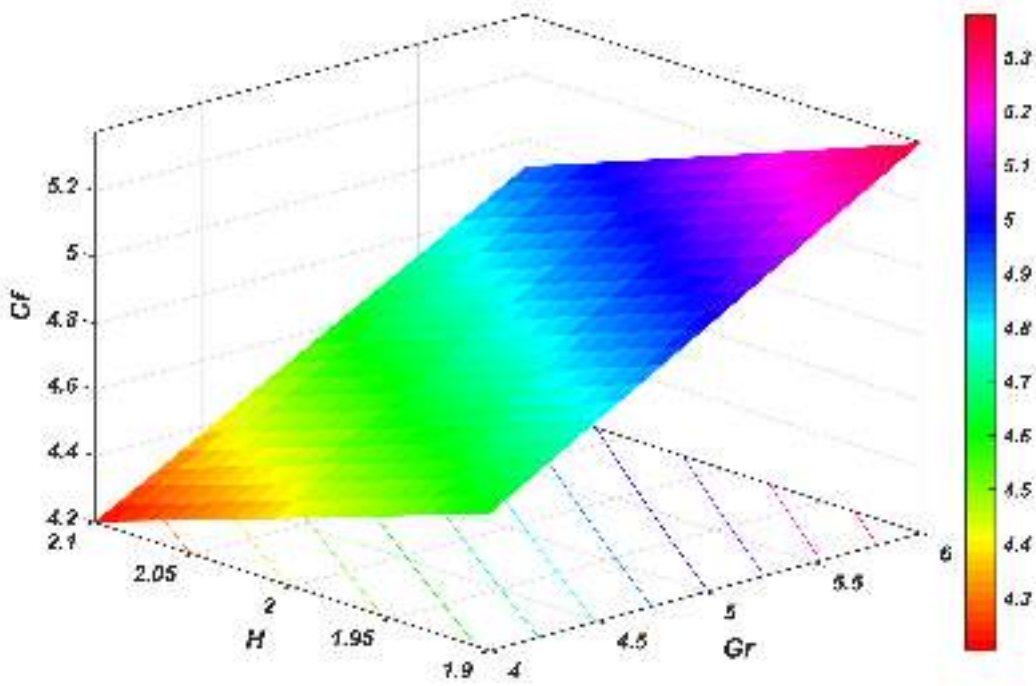


Figure 3.13: Variation in C_f with Gr and H at $y = 1$

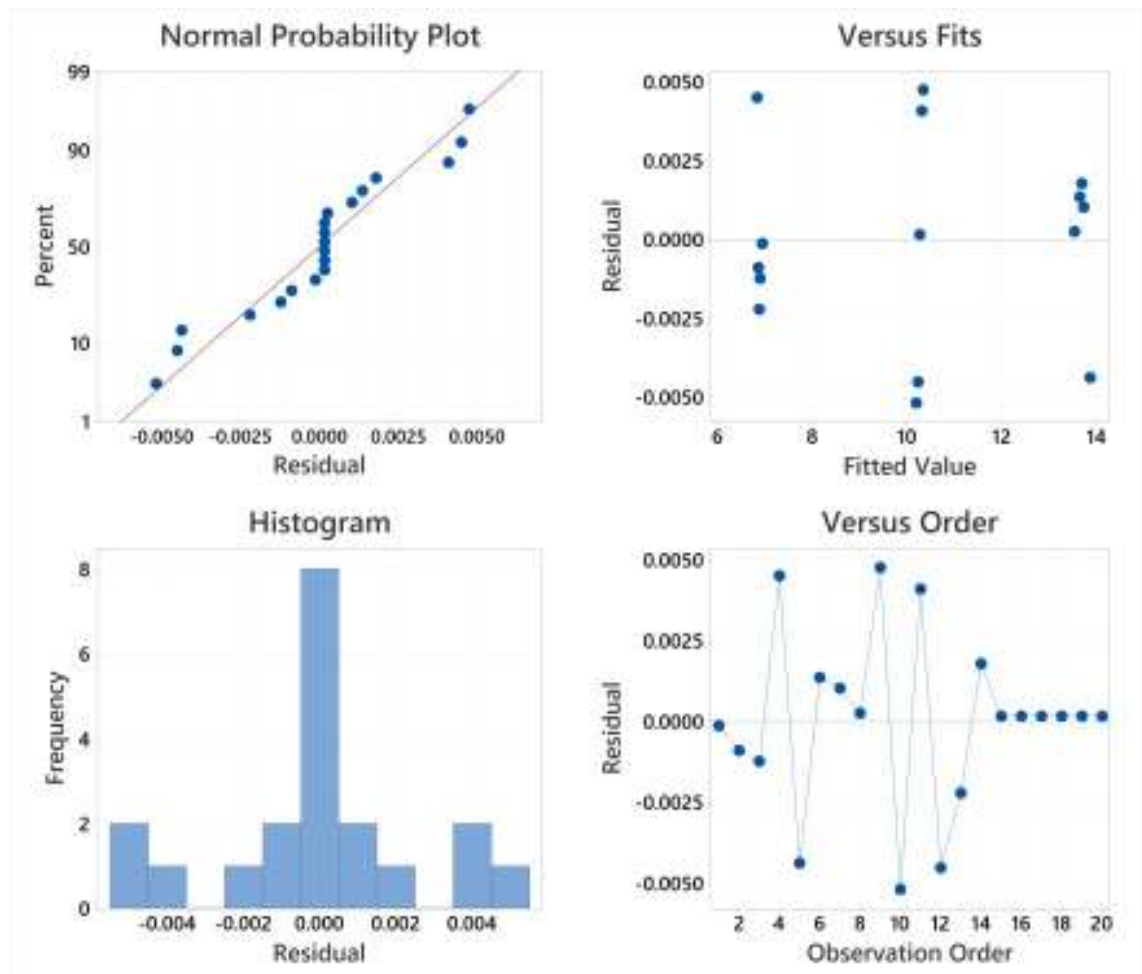


Figure 3.14: *Residual plots*

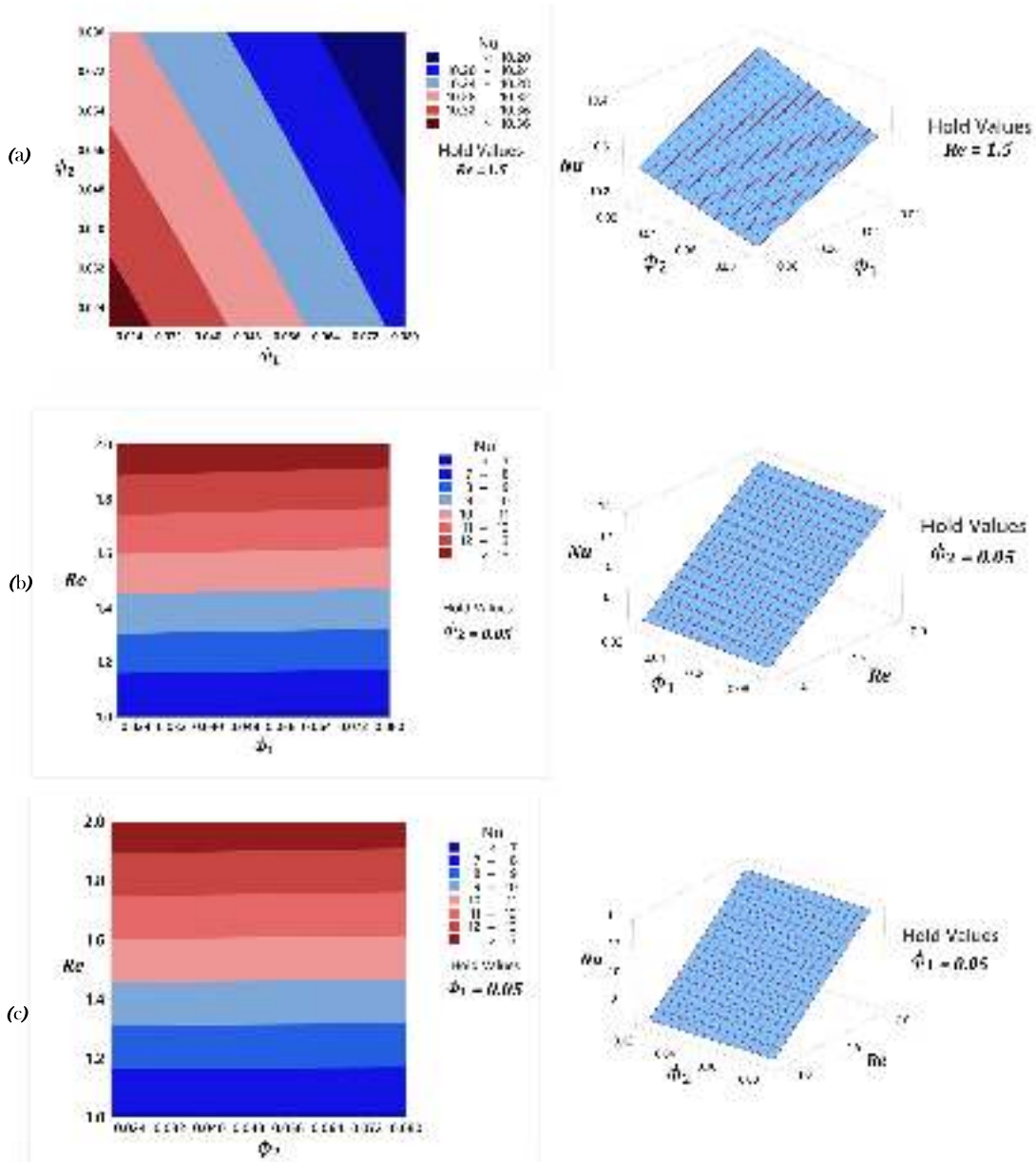


Figure 3.15: Contour and surface plots for Nu

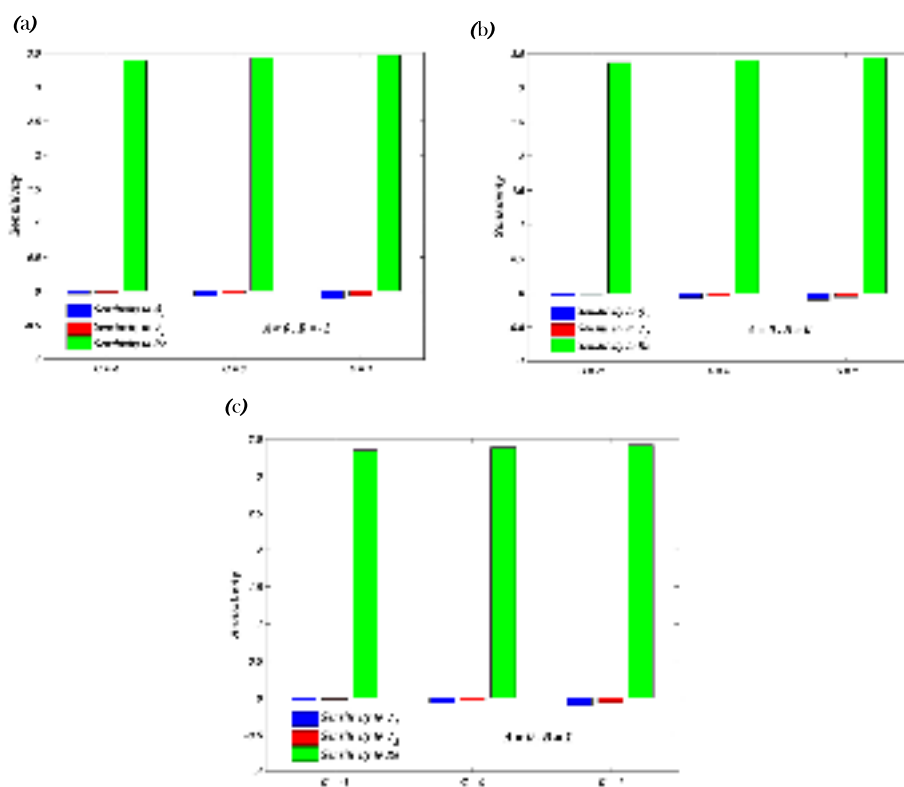


Figure 3.16: Bar charts depicting the sensitivity of Nu

Appendix I: Non-Dimensional Quantities

$$Pr = \frac{(\mu c_p)_f}{k_f} \quad \text{Prandtl Number}$$

$$Re = \frac{U_0 d}{\vartheta_f} \quad \text{Injection/ Suction Parameter}$$

$$H = B_0 d \sqrt{\frac{\sigma_f}{\rho_f \vartheta_f}} \quad \text{Hartmann Number}$$

$$Gr = \frac{g \beta_f \vartheta_f (T_0 - T_1)}{U_0^3} \quad \text{Grashof Number}$$

Appendix II: Nomenclature

u^*, v^*, w^*	Velocity components	T^*	Fluid temperature
V_0	Injection velocity	g	Acceleration due to gravity
t^*	Time	T_0, T_1	Reference temperature
p^*	Pressure	C_p	Specific heat at constant pressure
B_0	strength of magnetic field	U_0	velocity of the moving plates
σ	Electrical conductivity	ϕ_1	Volume fraction of Al_2O_3
d	Distance between the plates	ϕ_2	Volume fraction of Fe_3O_4
μ	Dynamic viscosity	ρ	Density
ν	Kinematic viscosity	ω^*	Angular velocity
K	Thermal conductivity	f	Base fluid
nf	Nanofluid	s_1	Al_2O_3 Nanoparticle
hnf	Hybrid nanofluid	s_2	Fe_3O_4 Nanoparticle
$\varepsilon_1, \varepsilon_2, \varepsilon_3$	Very small reference constants		

Appendix III: Short keys

$$a_1 = \frac{C_5 Pr Re}{C_6}$$

$$a_2 = \frac{\frac{C_5 Pr Re}{C_6} + \sqrt{\frac{C_5^2 Pr^2 Re^2}{C_6^2} + \frac{4C_5 Pr \omega i}{C_6}}}{2}$$

$$a_3 = \frac{\frac{C_5 Pr Re}{C_6} - \sqrt{\frac{C_5^2 Pr^2 Re^2}{C_6^2} + \frac{4C_5 Pr \omega i}{C_6}}}{2}$$

$$b_1 = \frac{C_1 C_2 Re + \sqrt{C_1^2 C_2^2 Re^2 + 4C_1 C_3 H^2}}{2}$$

$$b_2 = \frac{C_1 C_2 Re - \sqrt{C_1^2 C_2^2 Re^2 + 4C_1 C_3 H^2}}{2}$$

$$b_3 = \frac{C_1 C_2 Re + \sqrt{C_1^2 C_2^2 Re^2 + 4(i\omega C_1 C_2 + C_1 C_3 H^2)}}{2}$$

$$b_4 = \frac{C_1 C_2 Re - \sqrt{C_1^2 C_2^2 Re^2 + 4(i\omega C_1 C_2 + C_1 C_3 H^2)}}{2}$$

$$b_5 = \frac{C_1 C_2 Re + \sqrt{C_1^2 C_2^2 Re^2 + 4(C_1 C_3 H^2 + \pi^2)}}{2}$$

$$b_6 = \frac{C_1 C_2 Re - \sqrt{C_1^2 C_2^2 Re^2 + 4(C_1 C_3 H^2 + \pi^2)}}{2}$$

$$A_1 = \frac{C_1 C_2 C_4 Re^2 Gr}{(e^{a_1} - 1)(a_1^2 - C_1 C_2 Re \ a_1 - C_1 C_3 H^2)}$$

$$A_2 = \frac{C_1 C_2 C_4 Re^2 Gr \ e^{a_1}}{(e^{a_1} - 1)C_1 C_3 H^2}$$

$$A_3 = \frac{C_1 C_2 C_4 Re^2 Gr e^{a_3}}{(e^{a_2} - e^{a_3})(a_2^2 - C_1 C_2 Re \ a_2 - C_1 C_2 i\omega - C_1 C_3 H^2)}$$

$$A_4 = \frac{C_1 C_2 C_4 Re^2 Gr e^{a_2}}{(e^{a_3} - e^{a_2})(a_3^2 - C_1 C_2 Re \ a_3 - C_1 C_2 i\omega - C_1 C_3 H^2)}$$

$$\alpha_1 = -(A_1 + A_2)$$

$$\beta_1 = -(2 + A_1 e^{a_1} + A_2)$$

$$\alpha_2 = -(A_3 + A_4)$$

$$\beta_2 = -(A_3 e^{a_2} + A_4 e^{a_3})$$

$$r_1 = \frac{b_1 + \sqrt{b_1^2 + 4\pi^2}}{2}$$

$$r_2 = \frac{b_1 - \sqrt{b_1^2 + 4\pi^2}}{2}$$

$$r_3 = \frac{b_2 + \sqrt{b_2^2 + 4\pi^2}}{2}$$

$$r_4 = \frac{b_2 - \sqrt{b_2^2 + 4\pi^2}}{2}$$

$$\alpha_3 = -\sum_{i=1}^4 (A_{i1} + A_{i2} + A_{i3})$$

$$\alpha_4 = -\sum_{i=1}^4 (B_{i1} + B_{i2} + B_{i3})$$

$$\beta_3 = -\sum_{i=1}^4 (A_{i1} e^{(r_i + b_1)} + A_{i2} e^{(r_i + b_2)} + A_{i3} e^{(r_i + a_1)})$$

$$\beta_4 = -\sum_{i=1}^4 (B_{i1} e^{(r_i + b_1)} + B_{i2} e^{(r_i + b_2)} + B_{i3} e^{(r_i + a_1)})$$

$$D_1 = r_3 r_4 (e^{r_2+r_4} - e^{r_2+r_3}) + r_2 r_4 (e^{r_3+r_2} - e^{r_3+r_4}) + r_2 r_3 (e^{r_3+r_4} - e^{r_2+r_4})$$

$$D_2 = r_3 r_4 (e^{r_1+r_3} - e^{r_1+r_4}) + r_1 r_4 (e^{r_3+r_4} - e^{r_3+r_1}) + r_1 r_3 (e^{r_1+r_4} - e^{r_3+r_4})$$

$$D_3 = r_2 r_4 (e^{r_1+r_4} - e^{r_1+r_2}) + r_1 r_4 (e^{r_2+r_1} - e^{r_2+r_4}) + r_1 r_2 (e^{r_2+r_4} - e^{r_1+r_4})$$

$$D_4 = r_2 r_3 (e^{r_1+r_2} - e^{r_1+r_3}) + r_1 r_3 (e^{r_3+r_2} - e^{r_2+r_1}) + r_1 r_2 (e^{r_1+r_3} - e^{r_2+r_3})$$

$$D = D_1 + D_2 + D_3 + D_4$$

$$A_{i1} = \frac{b_1(\alpha_1 e^{b_2} - \beta_1) C_1 C_2 \operatorname{Re} D i}{(e^{b_2} - e^{b_1}) D [(r_i + b_1)^2 - C_1 C_2 \operatorname{Re}(r_i + b_1) - (C_1 C_3 H^2 + \pi^2)]}, \quad i = 1, 2, 3, 4$$

$$A_{i2} = \frac{b_2(\beta_1 - \alpha_1 e^{b_1}) C_1 C_2 \operatorname{Re} D i}{(e^{b_2} - e^{b_1}) D [(r_i + b_2)^2 - C_1 C_2 \operatorname{Re}(r_i + b_2) - (C_1 C_3 H^2 + \pi^2)]}, \quad i = 1, 2, 3, 4$$

$$B_{i1} = \frac{b_1((\alpha_1 + 2)e^{b_2} - (\beta_1 + 2)) C_1 C_2 \operatorname{Re} D i}{(e^{b_2} - e^{b_1}) D [(r_i + b_1)^2 - C_1 C_2 \operatorname{Re}(r_i + b_1) - (C_1 C_3 H^2 + \pi^2)]}, \quad i = 1, 2, 3, 4$$

$$B_{i2} = \frac{b_2((\beta_1 + 2) - (\alpha_1 + 2)e^{b_1}) C_1 C_2 \operatorname{Re} D i}{(e^{b_2} - e^{b_1}) D [(r_i + b_2)^2 - C_1 C_2 \operatorname{Re}(r_i + b_2) - (C_1 C_3 H^2 + \pi^2)]}, \quad i = 1, 2, 3, 4$$

$$B_{i3} = A_{i3} = \frac{a_1 A_1 C_1 C_2 \operatorname{Re} D i}{D [(r_i + a_1)^2 - C_1 C_2 \operatorname{Re}(r_i + a_1) - (C_1 C_3 H^2 + \pi^2)]}, \quad i = 1, 2, 3, 4$$